Manuscript n.: AP2106-1256.R2

Reflector Antennas Characterization and Diagnostics using a Single Set of Far-Field Phaseless Data and Crosswords-like Processing

R. Palmeri, G. M. Battaglia, A. F. Morabito and T. Isernia, *Fellow, IEEE*

***Abstract*— We introduce and discuss a new approach to the phase retrieval of fields radiated by continuous aperture sources having a circular support, which is of interest in many applications including the detection of shape deformations on reflector antennas. The approach is based on a decomposition of the actual 2-D problem into a number of 1-D phase retrieval problems along diameters and concentric rings of the visible part of the spectrum. In particular, the 1-D problems are effectively solved by using the spectral factorization method, while discrimination arguments at the crossing points allow completing the retrieval of the 2-D complex field. The proposed procedure just requires a single set of far field amplitudes (but for an additional bit of information) and takes advantage from up-to-now unexplored field properties. The developed technique is assessed in the case of reflector aperture fields.**

***Index Terms*—Antenna measurements, aperture antennas, inverse problems, phase retrieval, spectral factorization.**

I. Introduction

In reflector antennas, deviations of the actual surface from the ideal one caused by gravity, wind, load, and temperature play an important role as they imply a degradation of the antenna efficiency [1],[2]. In fact [1], the root mean square error (RMSE) deviation of the reflector surface from the ideal one should be less than $\lambda/15$ in order to obtain more than 50% aperture efficiency (λ being the operating wavelength). Therefore, the challenge is to retrieve the reflector shape in an accurate fashion, so that possible countermeasures can be adopted. In this respect, Rahmat-Samii introduced in [2] a simple and widely adopted model relating the reflector shape deformation to the phase of the aperture field. More recently, a deformation-amplitude relationship has also been introduced in [3]. In both cases it is argued that the knowledge of the aperture field allows providing the desired information on deformation.

Several approaches have been proposed for reflector surface diagnostics. In short, one can find strategies based on the processing of both amplitude and phase of the radiated far-field [4]-[8] as well as strategies exploiting just the far-field power pattern (see for instance [9]-[14]). In particular, by using Geometrical Optics (GO) and the aperture antennas theory, Leone and Pierri analyzed in detail in [9] the problem of determining the reflector antenna surface from far-field phaseless data. As a matter of fact, collecting phase measurements can be very difficult or excessively expensive with increasing frequencies [15]-[17], and hence the second kind of strategy is indeed of interest. Accordingly, the problem of the surface shape detection in reflector antennas can be conveniently linked to a Phase Retrieval (PR) problem [10],[13].

By considering an unknown complex function $f(\underline{x})$ and an operator $\mathcal{T}$ such that $F(\underline{k}) = \mathcal{T}[f(\underline{x})] = |F(\underline{k})|e^{j\angle F(\underline{k})}$, the PR problem deals with the determination of the complex quantity $F(\underline{k})$ starting from the knowledge of $|F(\underline{k})|$ plus some additional information [18].

A very popular approach for such a kind of problems has been given by Misell in [19] in the context of electron microscopy, and later adapted to reflector antennas [10]. As essentially all PR methods available in literature for antenna or other devices characterization (but for [17],[20]), the latter approach requires some diversity in the collected data (e.g., two or more probes, two or more measurement surfaces, defocusing conditions, or the like [21],[22]). While being conceptually simple and fast, this procedure may converge to a so-called 'false solution' [23] if the initial estimation of the aperture distribution is far from the ground truth. A common way to tackle this issue (at least from a practical point of view) is the so-called 'hybrid input-output' empirical strategy [24], which is widely adopted [25].

Another benchmark and well-assessed approach, based on global optimization, is proposed in [14]. However, since the computational complexity of global optimization-based procedures is expected to exponentially grow with the number of unknowns [26], it can prevent the actual attainment of the global optimum in case of very large sources.

Finally, different approaches to PR have been recently introduced by relying on the 'PhaseLift' strategy (see [27],[28] and references therein). Unfortunately, the latter has two

This work was supported in part by the Italian Ministry of University and Research under the PRIN research project "CYBER-PHYSICAL ELECTROMAGNETIC VISION: Context-Aware Electromagnetic Sensing and Smart Reaction", prot. 2017HZJXSZ.

R. Palmeri is with Institute for the Electromagnetic Sensing of the Environment of the National Council of Research (IREA-CNR), 80124 Napoli, Italy. G. M. Battaglia, A. F. Morabito, and T. Isernia are with Department of Information Engineering, Infrastructures, and Sustainable Energy, Università di Reggio Calabria, 89122 Reggio Calabria, Italy.

Authors are also with CNIT (Consorzio Nazionale Interuniversitario per le Telecomunicazioni), 43124 Parma, Italy.

Corresponding author: Tommaso Isernia (tommaso.isernia@unirc.it).

important drawbacks, i.e., the computational complexity (which grows very rapidly with the number of unknowns) as well as the capability of determining only one solution of the problem (while in many cases, including 1-D PR, the problem can admit multiple solutions) [17],[29].

As a contribution towards effective solution strategies for such a problem, we present in the following a novel approach to PR. Notably, by avoiding iterative procedures, it allows determining the globally-optimal solution by using just one set of far-field amplitude measurements and the knowledge of the source support (and some other minimal information, see below).

The proposed approach relies on three basic bricks.

The first, and more obvious one, is the aperture antenna theory, which allows for simple relationships amongst the aperture field and the corresponding far-field from one side, and the aperture field and the reflector deformations from the other side.

The second brick, related indeed to the previous one, is given by the expansions of the aperture field and its spectrum in terms of the so-called Orbital Angular Momentum (OAM) modes, where the spectrum is given by suitable Hankel transforms of the aperture field modes [30],[31].

The third (and more innovative) brick is a recent approach to PR problems introduced by the authors for the case of 2-D discrete signals (with particular attention to array antennas and hence periodic spectra) [29]. In the latter, an analogy between filling the rows and columns of the spectrum matrix and completing a 'crosswords' scheme is introduced and discussed. In particular, the approach in [29] first casts the 2-D PR as a combination of 1-D PR problems. Then, it finds in a deterministic fashion all the admissible solutions of each 1-D problem by means of the Spectral Factorization (SF) method [32],[33]. Finally, enforcing congruence and discrimination criteria amongst them, the approach determines the correct field behavior along the different (horizontal, vertical, and diagonal) strips covering the 2-D scenario.

As in [29], the approach presented herein also exploits the strategy of decomposing the 2-D PR into a number of 1-D problems and solving these latter through the SF method. However, differently from [29], we solve herein 1-D problems along circles and diameters (rather than horizontal, vertical, and diagonal strips) over the spectral plane. Such a choice, which was just briefly introduced in [34],[35][1], automatically allows a considerable reduction of the computational burden associated to the inherent combinatorial problem. Moreover, it allows taking full advantage from effective representations based both on OAM field modes [30] and the inherent expansions based on Singular Value Decompositions (SVD) [36] and bandlimitedness [37]. These representations lead to a simple initialization of the PR procedure as well as a considerable reduction of the number of cases to be considered when checking congruence amongst fields on diameters and circles, which is achieved by also exploiting a relevant (and up-to-now overlooked) property of the fields along circles of the spectral plane.

Once the spectrum has been determined in a number of circles and diameters, the overall scheme can be eventually completed by solving a fitting problem that takes into account both the starting data (i.e., the square amplitude of the far-field) and the samples of the complex spectrum which have already been retrieved. In so doing, the presence of a quadratic and positive-definite term allows (along the guidelines of [23],[38]) avoiding the occurrence of false solutions.

Notably, the capability to complete the overall PR procedure by exploiting a single set of measurements (i.e., no diversity is needed) is indeed a relevant asset, since it allows a great simplification in the measurement procedure and acquisition time [17]. Following [18], we tackle the problem as an inverse one where, starting from the square amplitude distribution (and additional information), we mean to retrieve the complex spectrum and possibly the source. Hence, in order to accurately represent the data, the square amplitude has to be sampled at a rate which is twice that of the complex spectrum.

The method is herein presented in case of generic planar continuous sources contained in a finite circular support and exhibiting no particular symmetries. By virtue of its generality, it applies to whatever related PR problem, so that similar tools may be applied to synthesis (rather than recovery) problems. As detailed in the Conclusions, the approach can also be extended to near-field and other scanning configurations.

The remainder of the paper is as follows. In Section II, we briefly recall some useful mathematical tools of interest for aperture antennas. Then, convenient representations for the aperture field and the corresponding spectrum are given in Section III. In particular, it is argued that the aperture field's spectrum can be represented as a trigonometric polynomial along any circle and diameter of the spectral domain, and some up-to-now overlooked properties of this kind of polynomials are given. Then, the theoretical uniqueness and expected performances of the procedure are discussed in Section IV. After that, the rationale of the proposed strategy is presented in Section V, while the procedure arising from the joint consideration of the basic approach and of the introduced properties, as well as a detailed discussion about limitations and possible improvements, are given in Section VI. Finally, Section VII is devoted to an application of the given concepts to the diagnostics of deformations of reflector antennas. Conclusions follow.

II. Some Useful Expansions and Formulation of the Problem

By the sake of simplicity, let us consider the case where the aperture field is purely polarized along the x' (or y') direction, x' and y' denoting the coordinates spanning the aperture plane. In such a case, it is simple to see from the aperture antenna theory [39] that the knowledge of the square amplitude of the far-field components $E_{\infty_\theta}(\theta,\phi)$ or $E_{\infty_\phi}(\theta,\phi)$, θ and ϕ respectively denoting the antenna elevation and azimuth angles, is equivalent to the knowledge

[1] In these latter, two phase measurements were anyway used, and no equations were given.

of the square amplitude of the Fourier transform of the aperture field components $E_x(x',y')$ or $E_y(x',y')$ in the visible part of the spectrum. Hence, assuming we can measure either $\left|E_{\infty_\theta}\right|^2$ or $\left|E_{\infty_\phi}\right|^2$, we can restrict our attention to the 2-D Fourier-transform relationship amongst the (scalar) aperture field, which is named $f(x',y')$ in the following, and the corresponding spectrum.

Then, let us consider a continuous aperture field f having a circular support of radius a, which is of interest in reflector antenna diagnostics and in many other cases[2]. By denoting with ρ' and ϕ' the radial and azimuth coordinates spanning the aperture, f can be expanded in a multipole series as (see [30] for more details):

$$f(\rho',\phi') = \sum_{\ell=-\infty}^{+\infty} f_\ell(\rho') e^{j\ell\phi'} \tag{1}$$

where:

$$f_\ell(\rho') = \frac{1}{2\pi}\int_0^{2\pi} f(\rho',\phi') e^{-j\ell\phi'} d\phi' \tag{2}$$

Then, by respectively denoting with k and ϕ the radial and azimuth coordinates spanning the spectral domain, the Fourier transform of the source (1) is equal to:

$$F(k,\phi) = \frac{1}{2\pi}\int_0^{2\pi}\int_0^{\infty} f(\rho',\phi')\, e^{-jk\rho' cos(\phi'-\phi)} \rho' d\rho' d\phi' \tag{3.a}$$

and hence, for our finite-dimensional source enclosed in a circle of radius a, the following relationship holds true:

$$F(k,\phi) = \frac{1}{2\pi}\int_0^{2\pi}\int_0^{a} f(\rho',\phi') e^{-jk\rho' cos(\phi'-\phi)} \rho' d\rho' d\phi' \tag{3.b}$$

The Fourier transform (i.e., the spectrum) of the source can also be expanded in a multipole series as:

$$F(k,\phi) = \sum_{\ell=-\infty}^{+\infty} F_\ell(k) e^{j\ell\phi} \tag{4}$$

where:

$$F_\ell(k) = \frac{1}{2\pi}\int_0^{2\pi} F(k,\phi) e^{-j\ell\phi} d\phi \tag{5}$$

Note that, since we are dealing with a finite-dimensional source, $F(k,\phi)$ is a bandlimited function, so that expansion (4) admits convenient truncations.

On the basis of the (polarization) assumptions above, let us now consider the problem of reconstructing the 2-D source $f(\rho',\phi')$ from the knowledge (e.g., measurements) of the square-amplitude distribution of its Fourier transform in the visible part of the spectrum, i.e., $k \le \beta$ (β being the wavenumber). To this end, let us denote by $\boldsymbol{\mathcal{B}}[\cdot]$ and * the operator respectively performing the square amplitude and complex conjugate operations, so that :

$$\boldsymbol{\mathcal{B}}[F(k,\phi)] = F(k,\phi)F^*(k,\phi) = |F(k,\phi)|^2 \tag{6}$$

Then, if $M^2(k,\phi)$ denotes the measured square-amplitude far-field distribution[3], the (auxiliary, see below) 2-D PR problem of interest can be stated as the determination of the 'correct' F distribution (say $\hat{F}$) such that:

$$\boldsymbol{\mathcal{B}}\left[\hat{F}(k,\phi)\right] = M^2(k,\phi) \tag{7.a}$$

subject to

$$\hat{F}(k,\phi)\ obeying\ representation\ (3.b) \tag{7.b}$$

so that (7.b) enforces the finite dimension of the source.

Note that retrieving the phase of F (in the visible part of the spectrum) and retrieving $f(\rho',\phi')$ are not exactly the same problem, as the whole spectrum (and not just its visible part) would be required in order to safely recover the source distribution. Also, let us note that, in case of noisy data, the measured square-amplitude distribution might not permit the exact fulfillment of problem (7) and hence, even if uniqueness issues (see below) are neglected, the problem is still ill-posed [36]. Indeed, in solving (7) one generally looks for some best fitting, rather than looking for an exact fulfilment [18].

III. Effective Representation for the Spectrum and the Source, and Further Useful Properties

A. Representing the spectrum and the source via OAM modes and SVD

To give an accurate representation of the spectrum, we can exploit the SVD of the radiation operator relating the source $f_\ell(\rho')$ to the corresponding spectrum component $F_\ell(k)$.

In fact, if (1) is substituted into (3.b), and then (4) is used, the contribution to the radiated field given by (5) can be written as:

$$F_\ell(k) = \int_0^a f_\ell(\rho') J_\ell(k\rho') \rho' d\rho' = H_\ell\{f_\ell(\rho')\} \tag{8}$$

wherein, as reported in [30], $J_\ell(\cdot)$ is the ℓ-th order Bessel function of the first kind, and the last expression denotes the ℓ-order Hankel transform [31] of $f_\ell(\rho')$ (which is in turn supposed to be zero for $\rho' > a$).

Then, equation (8) can be written in an operator form as:

$$F_\ell = A_\ell f_\ell \tag{9}$$

A_ℓ being a compact notation for the corresponding (radiation) operator.

We can now perform the SVD of A_ℓ, i.e., $\{v_{\ell,n}, \sigma_{\ell,n}, u_{\ell,n}\}$ such that:

$$A_\ell v_{\ell,n} = \sigma_{\ell,n} u_{\ell,n} \tag{10.a}$$

$$A_\ell^+ u_{\ell,n} = \sigma_{\ell,n} v_{\ell,n} \tag{10.b}$$

$\sigma_{\ell,n}$, $v_{\ell,n}$, $u_{\ell,n}$ denoting the n-th singular value, left-hand singular functions, and right-hand singular functions associated to the ℓ-th order, respectively, while A_ℓ^+ is the adjoint operator of A_ℓ. A detailed description on how to compute the functions and scalars at hand is given in [30].

Since the singular functions $v_{\ell,n}$ and $u_{\ell,n}$ are orthonormal in

[2] Obviously, any finite-dimensional planar source can be delimited by some circle having a sufficiently large radius.

[3] Note that, by virtue of the bandlimitedness of the field [37], the function $M^2(k,\phi)$ can be conveniently acquired through proper sampling and interpolation operations.

the space of sources and spectra [30],[36] respectively, they can be used as representation bases in the corresponding domains. Therefore, we can represent the different spectrum components as follows:

$$F_\ell(k) = \sum_{n=1}^{\infty} b_{\ell,n}\, u_{\ell,n}(k) \tag{11}$$

and, by substituting (11) into (4), we finally achieve:

$$F(k,\phi) = \sum_{\ell=-\infty}^{+\infty} \sum_{n=1}^{\infty} b_{\ell,n}\, u_{\ell,n}(k) e^{j\ell\phi} \tag{12}$$

Then, assuming the source is not superdirective, expansion (12) can be conveniently truncated by following the rules reported in [30]. By so doing, one achieves:

$$F(k,\phi) = \sum_{\ell=-\beta a}^{\beta a} \sum_{n=1}^{N_\ell} b_{\ell,n}\, u_{\ell,n}(k) e^{j\ell\phi} \tag{13}$$

where $N_0 = \frac{2a}{\lambda}$ and the generic value of N_ℓ is given by:

$$N_\ell = N_0 - \frac{|\ell|}{\pi} \tag{14}$$

Hence, starting from (13), a convenient representation for the aperture field, corresponding to a regularized inversion of the (visible part of the) spectrum to the source, is given by:

$$f(\rho',\phi') = \sum_{\ell=-\beta a}^{\beta a} \sum_{n=1}^{N_\ell} \alpha_{\ell,n}\, v_{\ell,n}(\rho') e^{j\ell\phi'} \tag{15}$$

with $b_{\ell,n} = \sigma_{\ell,n}\alpha_{\ell,n}$.

Notably, provided one is able to retrieve the visible part of the spectrum, (15) can be conveniently exploited in order to regularize the ill-posed problem of identifying the aperture source distribution corresponding to the retrieved visible part of the spectrum.

B. Trigonometric polynomial representation of the spectrum along rings of the data domain, and its properties with increasing radii

Spectrum and source representations even more convenient than (13) and (15) can be devised by exploiting the fact that the singular functions $u_{\ell,n}(k)$ exhibit a $|\ell|$-th order zero for $k = 0$. Hence, for $k = 0$ only the functions $u_{0,n}(k)$ contribute to the spectrum. Moreover, the smaller the value of k the smaller the value of ℓ up to which functions $u_{\ell,n}(k)$ play a significant role in the spectrum generation [30].

Accordingly, in (13) the external summation can be further truncated to the interval $[-H, H]$, where H depends both on a and k, i.e.:

$$F(k,\phi) = \sum_{\ell=-H(k,a)}^{H(k,a)} \sum_{n=1}^{N_\ell} b_{\ell,n}\, u_{\ell,n}(k) e^{j\ell\phi} \tag{16.a}$$

Therefore, when considering a ring of radius $k = \overline{k}$, the spectrum can be conveniently written in terms of a trigonometric polynomial whose order depends indeed on $\overline{k}$ (i.e., the lower $\overline{k}$, the lower the order of the polynomial). As a matter of fact, along a ring of radius $\overline{k}$ one can use:

$$F(\overline{k},\phi) = \sum_{\ell=-H(\overline{k},a)}^{H(\overline{k},a)} C_\ell(\overline{k}) e^{j\ell\phi} \tag{16.b}$$

As far as the actual choice of H is concerned, it could be deduced from the properties of the singular functions. However, a simpler yet accurate estimation of the (minimum) value of H to be used in (16) can be given as follows.

First note that, by virtue of the source size, the minimal sampling period in the spatial frequency domain is equal to $1/2a$. As a consequence, the sampling period along any line in the spectral domain is equal to π/a. Hence, along a circumference having a radius $k = \overline{k}$ one needs a number of samples equal to $(2\pi\overline{k})/(\pi/a) = 2\overline{k}a$. Then, by performing a trigonometric interpolation of these samples, one can transform the arising sampling series based on the Dirichlet kernel into a truncated Fourier series [40], finding that H must be greater than or equal to $\overline{k}a$.

The choice $H = \overline{k}a$, which we assume in the following, nicely agrees with (13) when $\overline{k} = \beta$, i.e., along the maximum circle of the visible space. In fact, $H(\beta, a) = \beta a$.

Notably, by obvious derivations, the square amplitude distribution of the spectra along rings can also be expressed as trigonometric polynomials whose order is exactly twice the one of the corresponding complex spectra. Such a circumstance also suggests a further (practical) rule for a convenient choice of H along any circle in the spectral domain. In fact, one can estimate the value of $2H$ directly from the square amplitude distribution available along the circle at hand.

Expressions (16) for the spectrum in terms of the singular functions (or, more simply, in terms of trigonometric polynomials) can be conveniently used in the proposed procedure. To this end, let us note that trigonometric polynomials of the kind (16.b) can also be seen as the restriction to the unitary circle of an expression of the following kind:

$$F(\overline{k},\phi) = \sum_{\ell=-H}^{H} C_\ell(\overline{k}) z^\ell \tag{17}$$

with $z = e^{j\phi}$.

It is also well known [41] that the complex zeroes of (17) determine the actual behavior of the spectrum [32]. In this respect, it is useful to get an understanding of the (number and) locations of these zeroes with increasing values of k, which corresponds to increasing values of H.

One can easily understand that such an order is nothing but zero when $k = 0$. Then, when k gently moves from the origin to larger values, the order of the polynomial also progressively increases, so that new zeroes come into play in the z-plane. Notably (see Appendix A) if one considers two nearby concentric circles with different radii such that the required value of H increases by one, and no zero occurs in the corresponding annulus of the spectrum, the two additional zeroes must necessarily be located one inside and one outside

the unitary circle in the z-plane[4]. Then, as long as the function $F(k,\phi)$ does not exhibit any zero in the disk $k<\overline{k}$, the trigonometric polynomial (17) exactly has half of the zeroes inside the unitary circle and the other half outside[5].

C. Trigonometric polynomial representation of the spectrum along diameters of the data domain

Convenient representations of the spectrum can also be given for fixed values of ϕ, i.e., along diameters of the circle corresponding to the visible region of the spectral plane.

If we assume that the spectrum is negligible in its invisible part, and that it is sufficiently small on its border (which is usually the case with reflector antennas), then the behavior of the spectrum along the diameter at hand can be accurately reconstructed from its Nyquist samples. Then, as any diameter of the visible space is shorter than the maximum circle by a factor π, one finds that the number of required samples is equal to $2\beta a/\pi = 4a/\lambda$, and the same statement holds true if we re-normalize the coordinate along the diameter by using $k' = k/2$, so that $-\pi \le k' \le \pi$. Finally, for any of the above diameters identified by $\phi = \overline{\phi}$, we can again use the correspondence amongst Dirichlet sampling series and truncated Fourier series [40] to come to the following expression:

$$F(k,\overline{\phi}) = \sum_{\ell=-2a/\lambda}^{2a/\lambda} \hat{C}_\ell(\overline{\phi}) z'^{\ell} \qquad (18)$$

with $z' = e^{\frac{jk}{2}} = e^{jk'}$ [6].

A more detailed explanation of (18) can be found in [42], where it is also argued that it may be convenient to slightly extend the summation in case of sources which are not so large with respect to λ. Roughly speaking, one can also argue that (18) is nothing but the field radiated by the original source as collapsed (according to the definition in [29],[43]) on the $\phi = \overline{\phi}$ line, and it is known [42] that the field radiated by a linear non-superdirective source can be seen as the field radiated by an equivalent 'virtual' array with a spacing equal to (or slightly smaller) than $\lambda/2$. In fact, (18) can also be seen as an array factor where the present k' replaces the usual spectral variable 'u'.

Again, the (complex) zeroes of (18) will determine the actual behavior of the spectrum [32], and of course the power pattern will have a similar expansion (with $4a/\lambda$ replacing $2a/\lambda$). Finally, since the source is supposed to be circular, the summation indices do not vary with the chosen line, i.e., with the value of $\overline{\phi}$. However, different indices could be conveniently used for different ϕ values in other cases (see Conclusions).

[4] Actually, they will be close to the origin and close to infinity, respectively, when beginning to come into play.

[5] If $F(k,\phi)$ exhibits instead one or more zeroes within the disk $k<\overline{k}$, one can eventually track the evolutions of the zeroes in the complex plane, thus determining (for any fixed value of $\overline{k}$) how many zeroes of the corresponding trigonometric polynomial are inside or outside the unitary circle of the z plane.

[6] Note such a choice implies that spanning a diameter corresponds to spanning the entire unitary circle in the z plane.

IV. Uniqueness And Other Relevant Issues

The rationale, scope, and capabilities of the proposed approach to 2-D PR are intimately related to relevant results regarding the uniqueness (or lack of uniqueness) for the considered problem in both the 1-D and 2-D cases. Hence, it is appropriate to briefly resume these results.

As a matter of fact, 1-D PR problems do not admit a unique solution. In fact, besides the 'trivial ambiguities' discussed below, the far-field square amplitude can be written (but for a constant) as the product of factors of the kind[7] $(e^{j\hat{u}} - z_i)$, $(e^{j\hat{u}} - \frac{1}{z_i^*})$ and any 'flipping' amongst each couple corresponds to a different solution[8] [32]. On the other side, by means of a well-defined procedure based on extracting (and pairing) the roots of the spectrum expression, one can determine all the possible solutions of the 1-D PR problems at hand. Therefore, for each 1-D PR problem we have a collection of possible solutions for the pertaining part of the spectrum.

As 2-D polynomials are not factorable (but for a zero-measure set of cases), ambiguities due to the spectral factorization do not generally occur in 2-D PR problems [17]. Accordingly, the solution of a number of 1-D PR problems and their correct intersection according to congruence and discrimination arguments allow achieving the actual solution, the only residual problem being the so called 'trivial ambiguities'. These latter are reported in the following:

(i) a constant phase on the spectrum, corresponding to the same constant phase on the aperture source;

(ii) a linear phase on the spectrum, corresponding to a translation of the source;

(iii) a conjugation of the complex spectrum, corresponding to a reversal (with respect to both axis) plus a conjugation of the source (i.e., of the aperture field in the problem at hand);

(iv) any combination of (i),(ii),(iii).

In fact, all the above situations result in the same identical square-amplitude field distribution.

The first two ambiguities can be successfully faced by respectively fixing a reference phase and supposing to know the support of the source. The third ambiguity keeps however there, and hence (even neglecting the zero-measure set of cases where the 2-D spectrum can be further factored) some additional a-priori information is needed in order to get a theoretically unique solution also in the 2-D case. However, the set of possible solutions is reduced to just a couple of possible solutions which are complex conjugate each of the other[9]. As detailed in Sect. VI, simple practical ways can solve this residual ambiguity and come to a unique solution.

By assuming that the required additional information is available, or when looking for all the different solutions in case of non-uniqueness, we still need a computational procedure able to get the ground truth (in case of uniqueness) or all the possible solutions (in case uniqueness does not hold true). As a matter of fact, because of false solutions [23], or

[7] $\hat{u} \equiv k/2$ along diameters, whereas $\hat{u} \equiv \phi$ along rings.

[8] Unless the two roots of the couple have unitary amplitude.

[9] Hence, a single bit of information can solve the residual ambiguity.

computational issues [17],[22],[38],[44], this is still an open problem in the literature, unless a number of independent measurements of the radiated field amplitude substantially larger than the one required for the theoretical uniqueness is used. This is actually the reason why in antenna diagnostics two different sets of (sufficiently-different) phaseless measurements [21],[22],[45]-[51] are usually assumed (but for our contributions [17],[29]).

V. Rationale of the Proposed Phase Retrieval Strategy: A Concentric Crosswords-like Scheme

Our proposed PR procedure, originally introduced for the case of array antennas in [29], is inspired by the solution of crosswords puzzles. These latter, which are quite diffused in every culture whose language adopts alphabets rather than ideograms, are indeed puzzles where vertical and horizontal words, subject to some (possibly ambiguous) definitions, have to correctly intersect. In fact, by virtue of bandlimitedness, the far-field matrix to be retrieved can be seen as a crossword scheme to be solved, so that the 2-D PR problem can be tackled as a collection of auxiliary 1-D PR problems along rows, columns, and diagonal lines.

Since we are dealing with circularly-supported aperture sources, and by virtue of the fact that it will bring a number of advantages, herein we will consider instead 1-D PR problems along rings and diameters of the spectral plane. For this reason, we refer to the present approach as to a 'concentric' crosswords-like scheme.

The approach overcomes relevant issues associated to our previous approach in [29]. In fact, in the latter, a horizontal, a vertical, and a diagonal cut of the far-field were needed in order to have three intersections and initialize the solution of the puzzle, resulting in a cumbersome combinatorial problem[10]. Notably, the 'concentric' scheme allows instead starting with just one ring and one diameter, hence considerably reducing the computational burden[11]. Moreover, and more important, further relevant advantages do occur (see Sections VI.B and VI.D below).

VI. The Proposed procedure

In the proposed procedure, one has to solve a sequence of 1-D problems and then use congruence arguments at the intersection points until the entire far-field matrix is retrieved. As already noticed, a substantial speed-up is however possible once solutions along a sufficient number of rings and diameters have been identified.

In the following, in subsection VI.A we briefly resume how to solve the 1-D PR problem, which is the basic brick for the overall procedure described in subsection VI.B. Then, subsections VI.C, VI.D, and VI.E discuss drawbacks of the basic procedure and the corresponding countermeasures and improvements allowed by the properties discussed in subsection III.B and [38]. Finally, the exploitation of the retrieved spectrum in order to determine the corresponding source is considered in subsection VI.F.

VI.A. A basic brick: 1-D Phase Retrieval via Spectral Factorization

Let us define with $\hat{u}$ the generic variable spanning the 1-D observation domain at hand, i.e.:

$$F(\hat{u}) = \begin{cases} F(k/2)\ for\ \phi = \overline{\phi} & (\text{i.e., for any diameter}) \\ F(\phi) \quad for\ k = \overline{k} & (\text{i.e., for any ring}) \end{cases} \tag{19}$$

Then, by using (17) or (18), and by obvious derivations [32], the square-amplitude distribution of (19) can be expressed in terms of auxiliary coefficients D_p such that:

$$|F(\hat{u})|^2 = S(\hat{u}) = \sum_{p=-2P}^{2P} D_p e^{jp\hat{u}} \tag{20}$$

where, according to contents of Section III, $P = H = \overline{k}a$ when $\hat{u} = \phi$ (i.e., for a ring) and $P = H = 2a/\lambda$ when $\hat{u} = k/2$ (i.e., for a diameter). Also note that, since the left-hand member is a real quantity, $\{D\}$ is a Hermitian sequence of $4P + 1$ complex coefficients, i.e., $D_p = D_{-p}^*$, $p = 0, 1, \dots, 2P$.

Then, by considering the measured square-amplitude data, i.e., M^2 as sampled in a grid of points $\mathbf{u} = [\hat{u}_1, \dots, \hat{u}_N]$, where N is the number of measurements taken according to [37], the Hermitian sequence $\{D_p\}$ can be identified by enforcing (in a least square sense) that:

$$\sum_{p=-2P}^{2P} D_p e^{jp\mathbf{u}} = M^2(\boldsymbol{u}) \tag{21}$$

Once the coefficients $\{D\}$ have been determined, the SF technique developed in [32] can be applied to get the multiplicity of solutions for any 1-D cut of the power pattern.

VI.B. An effective implementation for the conceived crosswords rationale

The rationale described in Section V could be implemented in many different ways. However, it is convenient dealing as much as possible with low-order polynomials. In fact, this allows an easier SF and, more important, a reduced number of possible solutions along the ring or diameter at hand. By following this general criterion, one comes to the procedure detailed in Appendix B.

In short, it proves convenient to initially (steps 1-5) consider a diameter and a small ring (such as for example the one at the Nyquist distance from the origin). Then, by using the SF, one can find all the possible behaviors along the diameter and the ring at hand. Note that, in order to be compatible, solutions on the two curves must have (but for some tolerance) the same phase shift at the two intersection points. Hence, one can discard all solutions along the diameter which are not congruent with any of the solutions on the ring (and vice versa). Also, it is fruitful keeping track of the surviving trial solutions, and of their diameter-ring solutions pairing.

Then (steps 7-11) a slightly larger ring can be considered,

[10] In fact, the first two intersections just normalize the phase along the second and third strip, and the third intersection allows for discrimination [29].

[11] In fact, they have two intersection points, the second one already allowing to discard incongruent solutions amongst the chosen diameter and ring.

and congruence arguments allow to further reduce the number of admissible solutions along the diameter. Notably, going back to the pairing of solutions amongst the diameter and the ring, solutions along the previous ring can also be pruned. As a consequence, the initial set of possible solutions along the initial couple diameter-ring is also pruned.

The procedure, allowing pruning along the chosen diameter and all the considered rings, can be repeated (step 12). As soon as the perimeter of the ring becomes equal to or greater than the diameter of the visible space, it proves convenient to switch to the consideration of a second diameter (step 13), and perform the SF therein. Notably, pruning of the set of solutions along such a line is very effective, as one can take profit from a number of discrimination points which is twice the number of considered rings. Also, such a congruence test will reduce the number of overall admissible solutions along the already-considered rings.

Further diameters can be then considered (steps 13-17).

As a final result, one will get all the different solutions of the problem at hand. In particular, in case the unknown spectrum is a non-factorable polynomial (which will always happen but for a zero-measure set of cases), at the end of the procedure one will get a couple of solutions respectively corresponding to the ground truth spectrum (or its best possible approximation) and its complex conjugate. Then, a single bit of additional information can solve the ambiguity. Practical additional information performing the job could be:

- a single phase shift measurement amongst two points;
- the knowledge of the (non-symmetric) support of the aperture source (in fact, conjugation of the spectrum corresponds to a source which is overturned with respect to the axes, and conjugated as well);
- other a-priori knowledge, such as for instance a quadratic phase component (with its sign) which is expected because of the chosen defocusing of the feed;
- knowledge of a sub-part of the aperture source (e.g., because of the blocking effects of the struts);

and further possibilities could be also devised.

In case the unknown spectrum is instead a factorable polynomial, because of its discrimination way of thinking the basic procedure will furnish in principle all the different solutions of the problem at hand, which could be a huge number. In such a case, which (luckily) is unlikely in the general case, the additional information which is needed for a unique solution implies additional a-priori information (or at least a part of a second set of data).

VI.C. Limitations of the approach

The proposed approach is affected from two main (related) limitations.

First, the presence of noise on data implies that one has to relax the requirements at the discrimination points. In fact, some tolerance has to be guaranteed when checking congruence in order to avoid discarding potential solutions along the different domains. As a consequence, more solutions may become admissible, and one may miss coming to the single couple of solutions which is expected, and finding instead more solutions. On the other side, let us note that whatever PR procedure using the same data would incur in the same kind of problem, as the solution(s) we find at the end are all compatible with the existing noisy data.

Second, the larger the source or the considered circle, the higher the order of the involved polynomials. As a consequence, one may have problems in the factorization[12] and, more important, one will have very many candidate solutions along the line (or the ring) at hand, so that many of them could be anyway admissible at the discrimination points, particularly in case of noisy data and hence larger tolerances.

In case of rings, let us note that if H is the index to be used in (17) (where H is proportional to k), then the corresponding square amplitude distributions have $4H$ possible zeroes, paired in couples of the kind $(z_i, 1/z_i^*)$ [32]. Then, without using any peculiar property of the spectrum, one should explore a total of 2^{2H} possible spectrum behaviors (as any of the $2H$ zeroes for the spectrum representation can be both inside or outside the unitary circle in the complex plane).

VI.D. Possible Improvements/1: exploitation of overlooked spectrum properties

Some interesting improvement in performance can be achieved by taking advantage of the properties discussed in Section III.B. In fact, by considering two nearby rings such that H has to be increased by one when moving from the smaller to the larger one, the two new zeroes must necessarily be located one inside and one outside the unitary circle, respectively. Such a circumstance implies that, amongst all the 2^{2H} possibilities above (and supposing for the time being that the spectrum does not exhibit any zero within the disk having the radius k at hand), the ones actually admissible are those where the inherent $2H$ zeroes are located half inside and half outside the unitary circle of the complex plane. Therefore, the number of combinations to be checked considerably reduces from 2^{2H} to the binomial coefficient $\binom{2H}{H}$, thus allowing a significant improvement in pruning the set of admissible solutions and computational effectiveness. Such a property can be exploited in all cases where no zero is present in the pattern over the disk of radius k. Once one or more zeroes are instead present within the above disk, one can focus the attention on the ring where transition occurs and 'track' the transition of the zeroes from inside to outside and vice versa, so that the number of situations to be checked is still much lower than 2^{2H}.

Interestingly, the possibilities of enhancing the PR procedure are not over yet. As a matter of fact, the 'zeroes tracking' idea can allow a further reduction of the complexity. In particular, if the 'zero tacking' procedure detailed in Appendix C is followed, by progressively enlarging the rings, the number of potential solutions to be explored follow a rule of the kind 2^H, which is a further relevant reduction.

[12] By using the subroutine 'roots' from Matlab we experienced some problems in correctly identifying (couples of) zeroes when the order of the polynomial is as high as 140 or more.

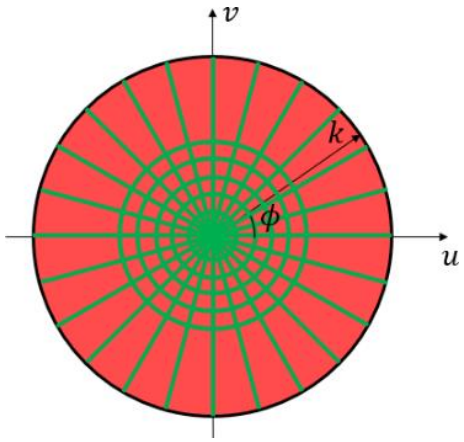

Fig. 1. Pictorial view of the field in the spectral domain before switching to the fitting procedure. At a certain step of the procedure detailed in Section VI.B and Appendix B, the complex field has already been retrieved along the green lines, while in the red zone it has yet to be recovered.

VI.E. Possible Improvements/2: a faster exploitation of partial results

At a certain step of the procedure detailed in Section VI.B and in Appendix B, the scenario at hand will appear as depicted in Fig. 1. In this figure, the retrieved spectrum is highlighted in green while the red part indicates those points where just the amplitude of the spectrum is known. Hence, to run out the PR procedure, we need to recover those points (or, better to say, the missing Nyquist samples).

Obviously, one can continue to consider additional diameters (or eventually rings). As an alternative strategy, advantage can be taken from [23],[38]. In these papers it is in fact shown that once a sufficiently large ratio amongst the number of independent square amplitude data and the number of independent unknowns is available, false solutions (corresponding to local minima of suitable cost functionals) can be avoided, and PR problems can be safely solved by local optimization techniques. In particular, it has been argued in [38] that once the ratio between the effective dimensions of the data space and the space of real independent unknowns is as large as 3, iterative procedures minimizing a cost function on the square amplitude data are not any more trapped into false solutions.

Herein, the recovered spectrum samples can be seen as constraints lowering the number of independent unknowns [38], so that the strategies (and procedures) explored and discussed therein can be conveniently applied. In so doing, one can take advantage from the minimally-redundant spectrum representation $(16.a)$ and enforce the already known spectrum behavior by means of penalty terms rather than by strict equality constraints.

Coming to detail, let us suppose splitting the spectral domain samples in two sub-sets, i.e.: $\widehat{\Pi} \equiv (\hat{k}, \hat{\phi})$ where the complex spectrum values have already been retrieved and $\widetilde{\Pi} \equiv (\tilde{k}, \tilde{\phi})$ where just amplitude data (i.e., $M^2_{\tilde{k},\tilde{\phi}}$) are known. The PR completion is then performed by solving the following optimization problem:

$$\min_{\boldsymbol{b}} \psi(\boldsymbol{b}) = w_1^2 \psi_1(\boldsymbol{b}) + w_2^2 \psi_2(\boldsymbol{b}) \tag{22}$$

where $\boldsymbol{b}$ is the vector containing the representation coefficients $b_{\ell,n}$, while w_1^2 and w_2^2 are positive constants properly weighting the two functionals ψ_1 and ψ_2. These latter, following [38], are defined as:

$$\psi_1(\boldsymbol{b}) = \left\| \frac{\left|F_{\tilde{k},\tilde{\phi}}\right|^2 - M^2_{\tilde{k},\tilde{\phi}}}{M_{\tilde{k},\tilde{\phi}}} \right\|^2_{\widetilde{\Pi}} = \sum_{\tilde{k}} \sum_{\tilde{\phi}} \frac{\left[\left|F_{\tilde{k},\tilde{\phi}}\right|^2 - M^2_{\tilde{k},\tilde{\phi}}\right]^2}{M^2_{\tilde{k},\tilde{\phi}}} \tag{23.a}$$

$$\psi_2(\boldsymbol{b}) = \left\| F_{\hat{k},\hat{\phi}} - T_{\hat{k},\hat{\phi}} \right\|^2_{\widehat{\Pi}} = \sum_{\hat{k}} \sum_{\hat{\phi}} \left| F_{\hat{k},\hat{\phi}} - T_{\hat{k},\hat{\phi}} \right|^2 \tag{23.b}$$

where $T_{\hat{k},\hat{\phi}}$, is the complex spectrum as retrieved by following the procedure described in Section VI.B.

Accordingly, the optimization problem (22) aims at determining coefficients $b_{\ell,n}$ such that the amplitude data, i.e., $M^2_{\tilde{k},\tilde{\phi}}$, are fitted through $(23.a)$, while $T_{\hat{k},\hat{\phi}}$, is fitted through $(23.b)$. Note that, while functional $(23.b)$ is quadratic with respect to unknowns, functional $(23.a)$ is indeed quartic.

To perform the optimization, a conjugate gradient-based minimization scheme is adopted. As well known, for a given starting guess, this kind of deterministic solution algorithm converges to the closest local minimum of the cost functional [52]. Therefore, thanks to the already retrieved portions of the spectrum and the presence of the corresponding positive definite quadratic functional $(23.b)$, one can avoid the occurrence of minima other than the global one [38].

VI.F Aperture Field Retrieval

While the PR problem can be considered accomplished at the end of the procedures described in Sections VI.B and VI.D and/or the solution of the optimization problem (22)-(23), the diagnostics problem we are interested in pursues the retrieval of the aperture field distribution (as it is the one actually conveying information about reflector shape deformations).

By virtue of the choice we have performed on the spectrum representation, such a last step can be performed in a simple fashion. In fact, once the complex spectrum is identified, $b_{\ell,n}$ coefficients are also known. Then, we can use (15) in order to determine the aperture field, where $\alpha_{\ell,n} = b_{\ell,n}/\sigma_{\ell,n}$. An even simpler solution, which can be safely applied whenever the spectrum is negligible in its invisible part (which is usually the case with reflector antennas) amounts to perform an inverse 2-D Fourier transform.

VII. Numerical Examples

The aim of this Section is to assess feasibility and effectiveness of the proposed approach in the diagnosis of surface deformations on a reflector antenna by not exploiting any phase measurement of the field. To this end, following [13], we have examined two different cases, namely the case where only the phase of the aperture field is affected and the

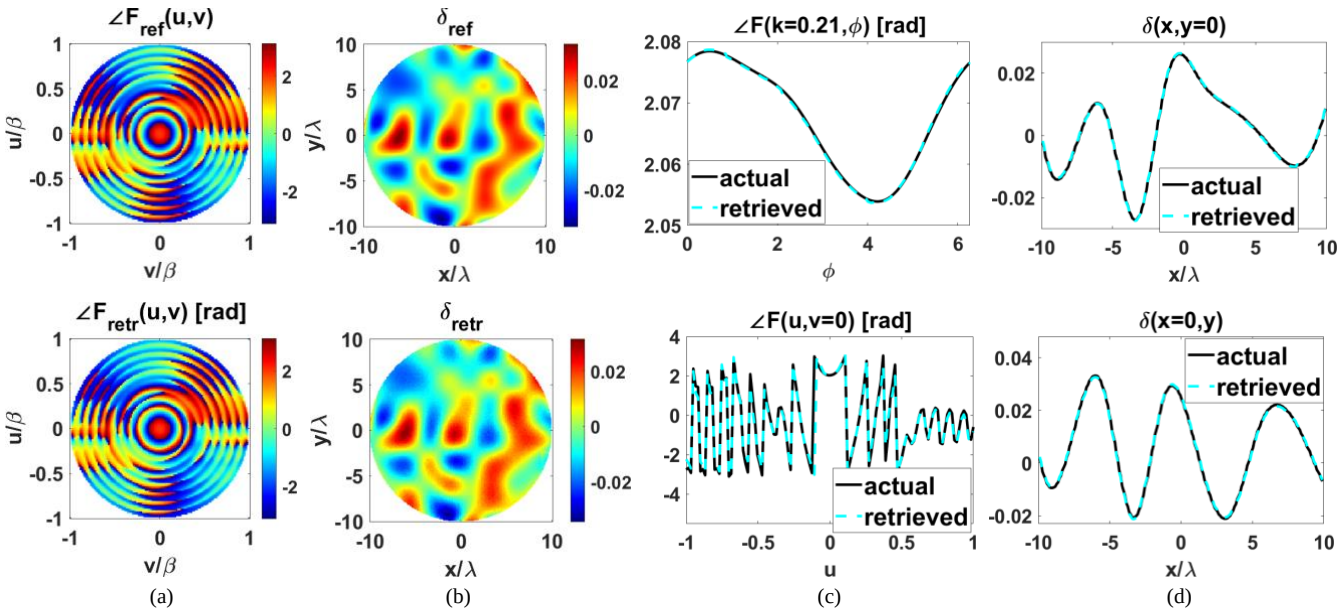

Fig. 2. Assessment scenario #1: phase distortion on aperture field ($u = k cos\phi$, $v = k sin\phi$). From left to right: (a) reference (top) and retrieved (bottom) phase of the radiated far-field; (b) reference (top) and retrieved (bottom) reflector surface deformation; (c) 1-D cuts of the reference (black curve) and retrieved (dashed-cyan curve) far-field phase along the ring at $k = 0.2094$ (top) and the diameter $v = 0$ (bottom); (d) 1-D cuts of the reference (black curve) and retrieved (dashed-cyan curve) surface deformation along $y = 0$ (top) and $x = 0$ (bottom).

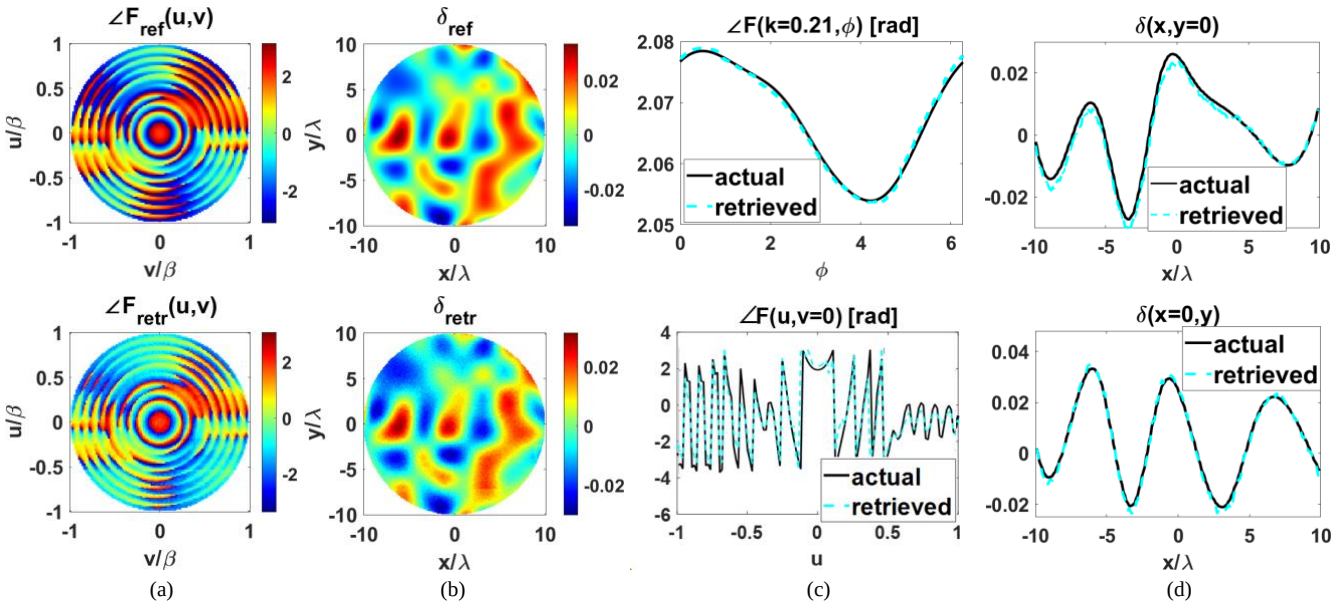

Fig. 3. Assessment scenario #1 in presence of noisy data (SNR=25dB): phase distortion on aperture field ($u = k cos\phi$, $v = k sin\phi$). From left to right: (a) reference (top) and retrieved (bottom) phase of the radiated far-field; (b) reference (top) and retrieved (bottom) reflector surface deformation; (c) 1-D cuts of the reference (black curve) and retrieved (dashed-cyan curve) far-field phase along the ring at $k = 0.2094$ (top) and the diameter $v = 0$ (bottom); (d) 1-D cuts of the reference (black curve) and retrieved (dashed-cyan curve) surface deformation along $y = 0$ (top) and $x = 0$ (bottom).

case where both the amplitude and the phase are affected.

As a reference scenario, we considered a continuous aperture field with a circular support of radius $a = 10\lambda$, whose nominal expression, corresponding to an undistorted reflector and an out of focus feed, is the following:

$$f(\rho', \phi') = |f| e^{j\varphi_f} \qquad (24.a)$$

$$|f| = \frac{4FL}{4FL^2 + \rho'^2} \qquad (24.b)$$

$$\varphi_f = \beta \left[2FL + \tilde{C} \left(\frac{4FL^2 - \rho'^2}{4FL} \right) \right] \qquad (24.c)$$

wherein FL is the focal length. In all the examples below, $FL = 3\lambda$, $\tilde{C} = 0.5$ and, as in [13], a gaussian taper has been superimposed to (24.b) in order to get an overall 12 dB ratio amongst values attained by the field at the origin and at the border of the disk source.

In order to quantitatively appraise the accuracy of the

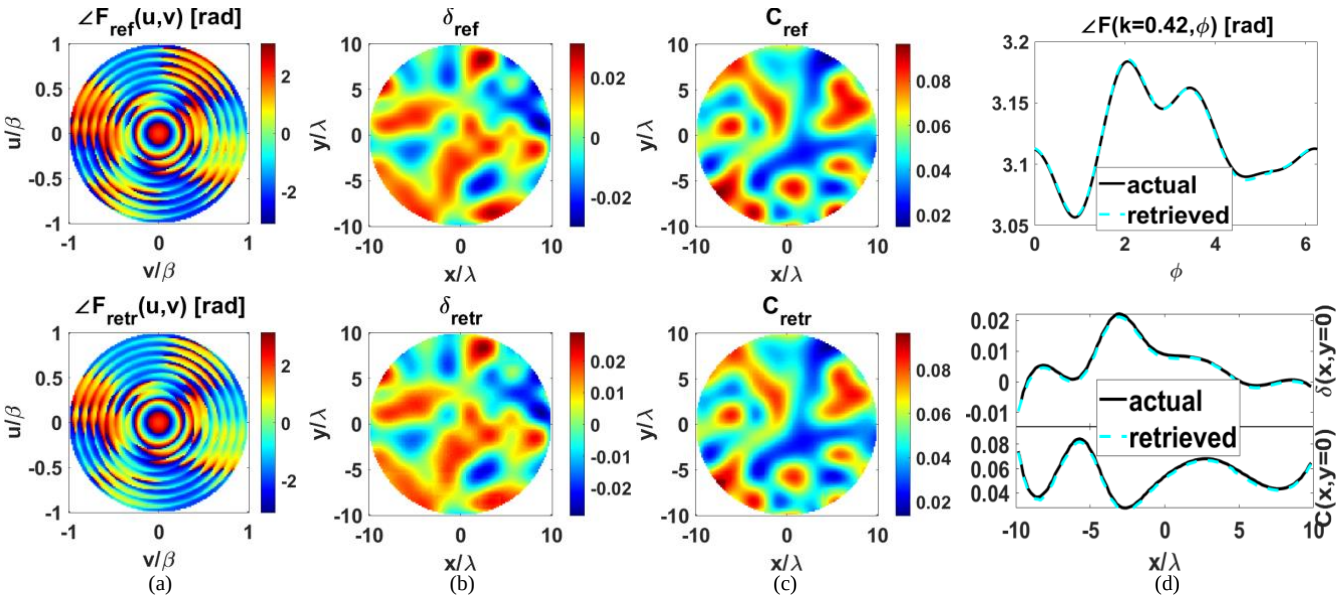

Fig. 4. Assessment scenario #2: amplitude and phase distortion on aperture field ($u = k cos\phi$, $v = k sin\phi$). From left to right: (a) reference (top) and retrieved (bottom) phase of the radiated far-field; (b) reference (top) and retrieved (bottom) reflector surface deformation; (c) reference (top) and retrieved (bottom) amplitude deformation; (d) 1-D cuts of the reference (black curve) and retrieved (dashed-cyan curve) far-field phase along the ring at $k = 0.4189$ (top) and surface and amplitude deformations along $y = 0$ (bottom).

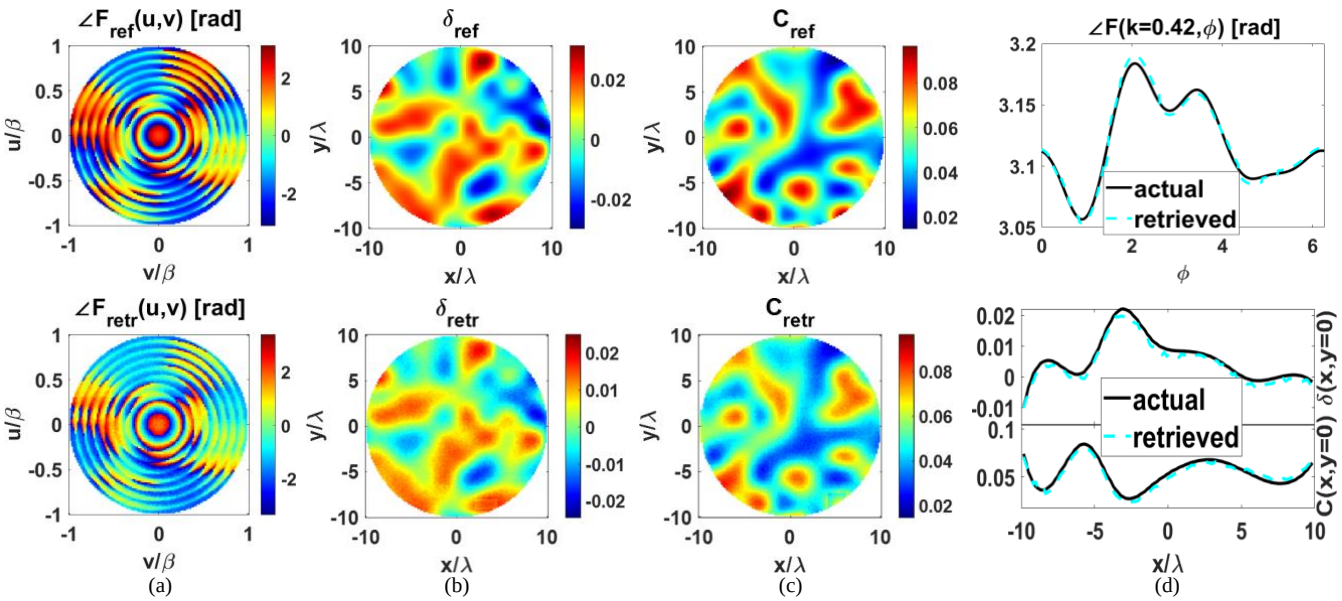

Fig. 5 Assessment scenario #2 in presence of noisy data (SNR=25dB): amplitude and phase distortion on aperture field ($u = k cos\phi$, $v = k sin\phi$). From left to right: (a) reference (top) and retrieved (bottom) phase of the radiated far-field; (b) reference (top) and retrieved (bottom) reflector surface deformation; (c) reference (top) and retrieved (bottom) amplitude deformation; (d) 1-D cuts of the reference (black curve) and retrieved (dashed-cyan curve) far-field phase along the ring at $k = 0.4189$ (top) and surface and amplitude deformations along $y = 0$ (bottom).

obtained results, we introduced a normalized square error (NSE) metric for both the radiated field (i.e., NSE_{rf}) and the surface deformation δ (i.e., NSE_{sd}) as follows:

$$NSE_{rf} = \frac{\|F^{actual}(k,\phi) - F^{recovered}(k,\phi)\|^2}{\|F^{actual}(k,\phi)\|^2} \qquad (25.a)$$

$$NSE_{sd} = \frac{\|\delta^{actual}(\lambda) - \delta^{recovered}(\lambda)\|^2}{\|\delta^{actual}(\lambda)\|^2} \qquad (25.b)$$

VII.A Phase distortion example

In the first example, besides the non-trivial behavior induced by (24.c), we also considered, as in [13], a surface deformation $\delta(\rho', \phi')$ on the reflector corresponding to a phase distortion of the aperture field as modeled in [2], that reads:

$$f(\rho', \phi') = |f| e^{j(\varphi_f + \Delta)} \qquad (26)$$

with:

$$\Delta = \frac{8FL^2\beta}{4FL^2 + \rho'^2}\delta \tag{27}$$

In order to set the same conditions, we fixed δ as randomly smooth in the range $\left[-\frac{\lambda}{30}, \frac{\lambda}{30}\right]$ according to the same rules as in [13].

By following the procedure reported in Appendix B, we started by initially considering the horizontal diameter and the first non-null ring at the Nyquist distance from the origin, i.e., $k = 0.157$. The solution of the corresponding 1-D PR problems led to 2^{14} and 2^3 possible solutions on the diameter and the ring, respectively. After fixing the reference phase at (k, ϕ)=(0.157, 0°), the congruence amongst solutions has been verified in (k, ϕ)=(0.157, 180°) by checking that the misfit on the unwrapped phase of trial solutions on diameter and ring is lower than 3°. As a consequence, only 62 and 4 solutions survived on the diameter and the ring, respectively.

Then, we considered the next ring at a Nyquist distance from the previous one and solved the pertaining 1-D PR problem, thus collecting 2^4 possible solutions. Once the reference phase has been set in order to get congruence at the (k, ϕ)=(0.314, 0°) point, the overall congruence amongst trial solutions has been checked at (k, ϕ)=(0.314, 180°). As a result, only 54 solutions survived along the diameter, and a pruning also occurred on the first ring by eliminating the solutions which were paired to the ones just withdrawn on the diameter. Then, we systematically proceeded by considering subsequent rings until the criterion relative to step 12 of the procedure described in Appendix B has been fulfilled, which in this case required the consideration of 8 rings. Then, we processed the subsequent diameters as described in steps 13-17 and achieved a single couple of complex conjugate solutions along each one-dimensional cut. Note that, in order to speed up the procedure, we exploited the first trick detailed in Subsection VI.D.

Once a sufficient number of field samples were achieved, we finally solved the fitting problem (22) by setting the weighting parameters w_1^2 and w_2^2 equal to the inverse of the energy of the pertaining data.

A comparison between the reference and one of the two final reconstructions of $F(k, \phi)$ (the other one being the complex conjugate) is given in Fig. 2 in terms of spectra [subplots (a)], and surface deformation [subplot (b)], respectively. As a matter of fact, a satisfactory PR solution has been achieved, as also witnessed by the cuts in Fig. 2 [subplot (c) and (d)] leading to $NSE_{rf} = 5.09 \cdot 10^{-4}$ and $NSE_{sd} = 6.15 \cdot 10^{-4}$.

By exploiting a PC equipped with an Intel i7-6700HQ CPU and 16 GB RAM, the numerical reconstruction required roughly three hours. As it can be seen, the approach has been able to retrieve not only the far-field phase, but also the aperture source amplitude and phase, including the term related to the reflector deformation [see subplot (d) of Fig. 2].

In the second example, the proposed PR strategy has been successfully tested in case of data corrupted by white gaussian noise with a given signal-to-noise-ratio (SNR) equal to 25dB.

As the 1-D PR problem solutions are affected by error, we enlarged the tolerance on the phase misfit to 15°, which implies more difficulties in pruning (as more solutions become admissible). However, the procedure again succeeded in finding the actual $F(k, \phi)$ (and its complex conjugate function), and the computational time only slightly increased.

The achieved results, corresponding to $NSE_{rf} = 7.91 \cdot 10^{-3}$ and $NSE_{sd} = 8.09 \cdot 10^{-3}$, are shown in Fig. 3, and confirm the effectiveness of the proposed PR approach also in presence of noise on data. In fact, one is able to come to a fully satisfactory reconstruction of the radiated field as well as of the overall aperture deformation.

VII.B Amplitude and Phase distortion example

As a second assessment scenario, we simulated a distortion on *both* the amplitude and the phase of the aperture field. In particular, we assumed that the surface deformation $\delta(\rho', \phi')$ [13] causes a phase distortion on $f(\rho', \phi')$ together with an increase $C(\rho', \phi')$ [13] in the amplitude, i.e.:

$$f(\rho', \phi') = |f|(1 + C)e^{j(\varphi_f + \Delta)} \tag{28}$$

As in [13], we set C randomly smooth such that $0 < C < 0.1$ [see Fig. 4(c)].

The PR procedure led to applying the 1-D PR via SF to the same rings and diameters of the previous example, by adopting also the same tolerance for the phase misfit.

The outcomes of the fitting problem for one of the two final solutions can be seen in Fig. 4 in terms of spectra [subplots (a)] and surface deformation [subplot (b) and (c)]. As it can be seen, the proposed method led again to a fully satisfactory recovery, which is testified by the very low values of the $NSE_{rf} = 4.23 \cdot 10^{-4}$ and $NSE_{sd} = 7.05 \cdot 10^{-4}$. This numerical example required a computational time close to that of the previous examples.

As last test case, we used the same scenario but enhanced the PR difficulty by corrupting each measured amplitude with SNR=25dB. A comparison between the reference and the reconstruction is given in Fig. 5 in terms of spectra [subplots (a)] and surface deformation [subplot (b) and (c)]. By adopting again a tolerance equal to 15° for the phase misfit, a satisfactory PR solution has been achieved as testified by Fig. 5 as well as $NSE_{rf} = 8.03 \cdot 10^{-3}$ and $NSE_{sd} = 9.12 \cdot 10^{-3}$.

In all the examples, we exactly followed the prescribed unambiguous steps defined in Appendix B. A full automation of the overall code is in progress.

VIII. CONCLUSIONS

A new general approach to the canonical problem of reconstructing 2-D spectra starting from amplitude measurements has been proposed and discussed.

The proposed technique, which also aims at recovering the corresponding aperture sources, jointly exploits a number of theoretical and methodological tools including recent expansions based on OAM modes and SVD, the overlooked spectral factorization method, and a crosswords-inspired processing.

By complementing all the above with the analysis and exploitation of the zeroes of the trigonometric polynomials expressing the spectrum and its square amplitude along

diameters and rings, the proposed procedure brings decisive useful characteristics with respect to the state-of-the-art approaches under different aspects. In fact, differently from essentially all the available phase retrieval procedures, the presented one just requires a single measurement set (plus the knowledge of the support of the source or some other minimal a-priori information), with relevant advantages in terms of cost, reliability, and effectiveness.

Such a result is achieved by taking joint advantage from theoretical circumstances as well as an original way of exploiting the available data. In fact, by virtue of 2-D bandlimitedness, discrimination arguments of the kind in [53] can be fruitfully used within the same set of data, rather than exploiting a second set of data. Moreover, in comparison with more usual approaches based on the minimization of cost functionals, we exploit herein a different discrimination procedure.

The price which is paid is a considerable increase in computational burden with respect to procedures based on the minimization of a cost functional. However, the strategy presented herein (as compared to the one in [29]) as well as the (up-to-now overlooked) properties of the field along rings presented in Section III allows very relevant savings.

The actual capability to retrieve the complex aperture field distribution has been assessed in the detection of shape deformations on reflector antennas. However, any aperture antenna can be considered.

Of course, the approach is best suited for the case of sources having a circular shape, but it can also be applied to (for example) planar arrays on a rectangular grid[13]. In that case, one will use the superposition of the effects (and possibly the array factor) rather than the SVD expansion in going back from the spectrum to the source.

Obviously, as long as one can define a finite-dimension planar aperture such that the field is negligible outside it, one can also define a (minimum dimensions) circular aperture enclosing the actual aperture, and proceed along the same steps. As an alternative, in case of elliptical planar apertures, one can take into account the apparent dimensions of the source along any diameter of the spectral plane [43]. By so doing, one can use a less dense sampling along the diameters of the spectral plane parallel to the 'short' dimensions, thus reducing complexity of factorization of the corresponding polynomial and the number of solutions to be checked along the line at hand.

Notably, as the technique is essentially based on bandlimitedness of the source, and the fields keep bandlimited whatever the (finite-dimensional) source [37], the basic approach can be also extended to other kind of sources.

Our interest to the problem started from the case of radio telescopes [10],[54]. In fact, with respect to the amplitude and phase configuration [54], where unmodulated beacons from geostationary satellites are used for measuring amplitude and phase in the receiving mode, phaseless techniques allow to compensate for possible turbulence effects or position uncertainties affecting phase measurements. However, many different antennas related problems may benefit from the proposed approach and procedures. In this respect, extension to near-field measurements is a very interesting possibility. As a matter of fact, the theory of 'reduced radiated fields' by Bucci and co-workers [37],[55] demonstrate that near-fields (and their square amplitudes) can also be safely sampled along suitable auxiliary coordinates (i.e., they are bandlimited in terms of these auxiliary variables). Then, Shelkunoff-like [41] representations of the kind (17) and (18) can still be exploited, and in case of near-field measurements on a plane one can use essentially the same phase retrieval procedure as in the present paper, the additional difficulty being possible truncation errors. Moreover, one can intersect different circles for the spherical scanning, and in both cases advantage can be taken from bandlimitedness (in the auxiliary variables if needed) and the above procedures.

The main limitation of the proposed technique is related to the actual capability of dealing with larger and larger sources, and work on this issue is in progress. In fact, it is expected that a full exploitation of the basic ideas, of all the discussed possible improvements, and of the hybridization of the proposed approach and tools with other methods will further boost the effectiveness and interest of the proposed technique.

APPENDIX A
PROPERTIES OF SPECTRUM ZEROES BY MOVING ALONG RINGS WITH INCREASING RADIUS

The aim of this Appendix is to show an important and useful property concerning the zeroes of the spectrum along a given ring of the spectral plane. To this end, let us consider the polynomial representation (17) for the spectrum. For $k = 0$, it particularizes as:

$$F(0, \phi) = C_0 \tag{A.1}$$

where we can assume $C_0 = 1$ for the sake of simplicity. Then, let us suppose to move to a ring *in the close proximity* of the previous one, that is $k = \varepsilon$ (ε denoting a real and positive small number). In this case, we expect that:

$$F(\varepsilon, \phi) = \sum_{\ell=-1}^{1} C_\ell \, z^\ell \tag{A.2}$$

with $z = e^{j\phi}$, i.e., the spectrum representation admits two zeroes, z_1 and z_2. Accordingly, (A.2) can be re-written as follows:

$$F(\varepsilon, \phi) = C_0 (z - z_1)\left(\frac{1}{z} - \frac{1}{z_2}\right) \tag{A.3}$$

For ε sufficiently small, the spectrum behavior has to keep almost unchanged, i.e.:

$$\begin{aligned} (z - z_1)\left(\frac{1}{z} - \frac{1}{z_2}\right) &\approx C_0 = 1 \\ 1 - \frac{1}{z_2} e^{j\phi} - z_1 e^{-j\phi} + \frac{z_1}{z_2} &\approx 1 \end{aligned} \tag{A.4}$$

which just holds true if $z_1 \to 0$ and $|z_2| \to \infty$.

[13] Note the recent brief contribution [35] (where no theoretical analysis or equations is present) already provides examples dealing with planar arrays.

By supposing that zeroes gently vary by moving along rings having an increased radius, and that no zero is present in the pattern over the disk of radius k (otherwise the two zeroes degenerate to a zero having multiplicity equal to two and lying on the unitary circle of the complex plane), the same arguments can be applied by gradually increasing the radius (and the corresponding number H of harmonics).

As a consequence, result (A.4) allows asserting that the couples of zeroes progressively coming into play by increasing the radius of the ring emerge from zero and infinity, respectively. Hence, in the lack of zeroes inside the disk contained within the ring at hand, the zeroes of the spectrum along the ring at hand are located half inside and half outside the unitary circle of the complex plane.

APPENDIX B
THE PROPOSED PR PROCEDURE STEP-BY-STEP

The aim of this Appendix is to list the different steps of the proposed PR procedure, i.e.:

1. consider initially a diameter and a small ring, for example the one at a Nyquist distance (for the spectrum) from the center;
2. find all possible spectrum behaviors along the diameter and the ring. In order to get rid of problems arising with possible phase constants, fix the phase reference in such a way that the phase at the diameter-ring first intersecting point is zero;
3. check for congruence amongst the trial solutions along the diameter and along the ring. In order to be compatible, solutions on the two curves must have the same phase (but for some tolerance) at the diameter-ring second intersecting point;
4. discard all trial solutions along the diameter which are not congruent with any of the solution along the ring. In a dual fashion, discard all trial solutions along the ring which are not congruent with any of the solutions on the diameter;
5. keep track of the couples of admissible solutions. Note that, at this stage, the number of possible solutions along the diameter usually results (largely) decreased with respect to the initial number, and the same statement holds true for the ring;
6. consider a further (slightly larger) ring, and find all possible field solutions;
7. fix the phase constant along the ring at hand in such a way that the phase at the first intersection points is the same as the one of the corresponding trial solution along the diameter;
8. check congruence of these solutions with the residual trial solutions on the diameter. In order to be compatible, solutions on the two curves must have the same phase (but for some tolerance) at the second intersection point;
9. discard all residual trial solutions along the diameter which are not congruent with any of the solutions along the ring at hand. In a dual fashion, discard all trial solutions along the ring which are not congruent with any of the residual trial solutions on the diameter;
10. go back to the previously considered rings and discard all solutions linked to the solutions on the diameter which have been just eliminated;
11. keep track of the overall (diameter plus considered rings) surviving trial solutions;
12. repeat steps 6-11 for rings having an increasing radius until the circumference of the ring equals the value of the diameter of the visible part of the spectrum (i.e., $k \leq 1$). Note these steps allows a subsequent pruning of the set of trial solutions along the diameter (see step 9) and the rings (see step 10);
13. consider a further diameter having the maximum possible angular distance with respect to the already considered ones, and find all possible spectrum solutions along it. For all of them, fix the phase reference in such a way that the phase in the origin is equal to the one determined along the first diameter;
14. check congruence of these solutions along the diameter at hand with the present set of overall possible solutions along the considered rings. Note in such a step one takes profit from a number of intersections (discrimination points) which is twice the number of the considered rings;
15. discard solutions on the diameter which are not compatible with any of the present overall trial solutions;
16. update the set of overall admissible trial solutions;
17. repeat steps 13-16 until one covers the overall spectral plane at the Nyquist rate. As an alternative, if just a couple of trial solutions survives and a sufficiently large number of spectrum samples has been retrieved according to the rules in [38], switch to a best-fitting procedure starting from one of them.

APPENDIX C
A 'ZERO-TRACKING' POSSIBLE PROCEDURE

To explain the idea of 'zero-tracking', let us consider a ring where just $H = 1$ is needed (which happens for a sufficiently small k). In this case, four zeroes are present in the square-amplitude distribution polynomial representation, say z_1, $1/z_1^*$, z_2, $1/z_2^*$[14].

On the basis of the considerations above, the number of possible corresponding spectrum behaviors on such a ring is given by the binomial coefficients described in Section VI.D and is equal to 2. In particular, they are associated to the two pairs of zeroes $\{z_1, 1/z_2^*\}$ and (its reciprocal and conjugate) $\{1/z_1^*, z_2\}$.

Then, suppose to consider the next ring and that, along it, the spectrum representation requires $H = 2$. In this case, four additional zeroes are present in the square-amplitude distribution beyond the initial ones, which have gently moved from their original positions in the complex plane. Let us denote by z_3, $1/z_3^*$, z_4, $1/z_4^*$ these additional zeroes. Again, by virtue of the spectrum properties, only the couples $\{z_3, 1/z_4^*\}$ and $\{1/z_3^*, z_4\}$ are actually admissible.

[14] Without any loss of generality, we assume that z_i is within the unitary circle while $1/z_i^*$ is outside it.

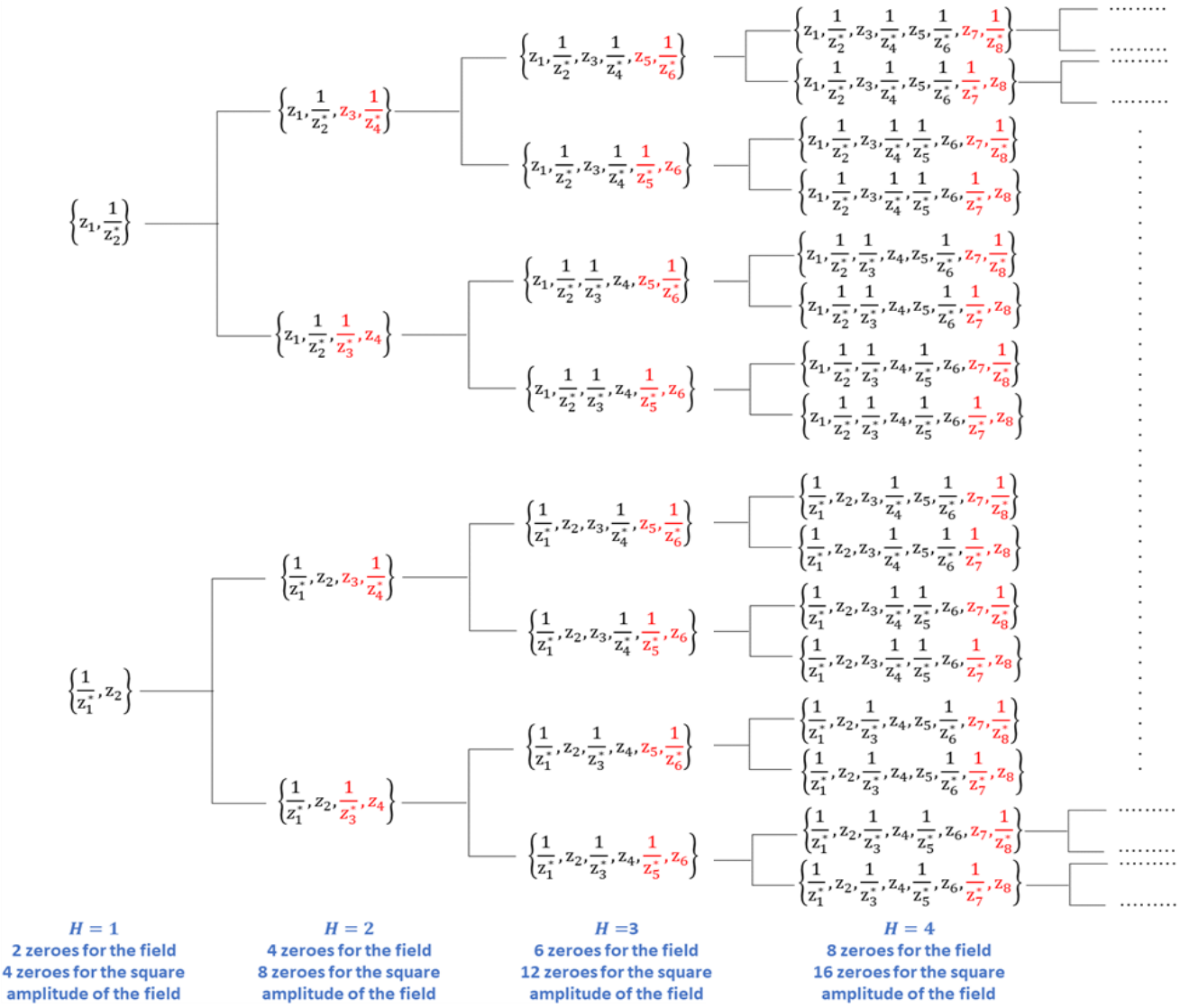

Fig. 6. Bifurcation tree of location of the zeroes when increasing the radius of the ring according to contents of Appendix C.

It follows that each of the initial two solutions 'bifurcates' in two new solutions. Notably, the same kind of reasoning applies when further increasing the radius of the considered ring. An illustrative representation of the bifurcation tree for increasing H values is shown in Fig. 6.

REFERENCES

[1] J. Ruze, "Antenna tolerance theory—A review," *Proceedings of the IEEE*, vol. 54, n. 4, pp. 633-640, 1966.

[2] Y. Rahmat-Samii, "Microwave holography of large reflector antennas - Simulation algorithms," *IEEE Transactions on Antennas and Propagation*, vol. 33, n. 11, pp. 1194-1203, 1985.

[3] J. Huang, H. Jin, Q. Ye, G. Meng, "Surface deformation recovery algorithm for reflector antennas based on geometric optics," *Optics Express*, vol. 25, n. 20, pp. 24346-24361, 2017.

[4] J. Bennett, A. Anderson, P. McInnes, and A. Whitaker, "Microwave holographic metrology of large reflector antennas," *IEEE Transactions on Antennas and Propagation*, vol. 24, n. 3, pp. 295-303, 1976.

[5] P. F. Scott, M. Ryle, "A rapid method for measuring the figure of a radio telescope reflector," *Monthly Notices of the Royal Astronomical Society*, vol. 178, n. 4, pp. 539-545, 1977.

[6] M. P. Godwin, A. J. T. Whitaker, J. C. Bennett, and A. P. Anderson, "Microwave diagnostics of the Chilbolton 25M antenna using the OTS satellite," *Proceeding of 2nd International Conference of Antennas and Propagation*, pp. 232-236, 1981.

[7] C. E. Mayer, J. H. Davis, W. L. Peters, and W. J. Vogel, "A holographic surface measurement of the Texas 4.9-m antenna at 86 GHz," *IEEE Transactions on Instrumentation and Measurement*, vol. 32, n. 1, pp. 102-109, 1983.

[8] G. Mazzarella, G. Montisci, and G. Serra, "A microwave holographic procedure for large symmetric reflector antennas using a Fresnel-zone field data processing," *International Journal of Antennas and Propagation*, vol. 2012, 2012.

[9] G. Leone, R. Pierri, "Reflector antenna diagnosis from phaseless data," *IEEE Transactions on Antennas and Propagation*, vol. 45, n. 8, pp. 1236-1244, 1997.

[10] D. Morris, "Phase retrieval in the radio holography of reflector antennas and radio telescopes," *IEEE Transactions on Antennas and Propagation*, vol. 33, n. 7, pp. 749-755, 1985.

[11] R. K. Amineh, J. McCombe, and N. K. Nikolova, "Microwave holographic imaging using the antenna phaseless radiation pattern," *IEEE Antennas and Wireless Propagation Letters*, vol. 11, n. 1, pp. 529-1532, 2012.

[12] Y. Xu, Q. Ye, and G. Meng, "Optimisation of phase factor in phase retrieval for reflector antennas with active surface," *IET Microwaves, Antennas and Propagation*, vol. 12, n. 15, pp. 2285-2291, 2018.

[13] H. Jin, J. Huang, Q. Ye, G. Meng, B. Xiang, and N. Wang, "Surface shape detection with a single far-field intensity by combined amplitude

and phase retrieval," *International Journal of Antennas and Propagation*, vol. 2019, 2019.

[14] A. Capozzoli, G. D'Elia, "Global optimization and antenna synthesis and diagnosis, part two: applications to advanced reflector antennas synthesis and diagnosis techniques," *Progress In Electromagnetics Research*, vol. 56, pp. 233-261, 2006.

[15] Y. Munemasa, T. Takano, M. Mita, and M. Sano, "Measurement of lightwave antennas: difficulties and peculiarities in comparison with radio-wave antennas," *IEEE Transactions on Antennas and Propagation*, vol. 55, n. 11, pp. 3040-3045, 2007.

[16] Y. Shechtman, Y. C. Eldar, O. Cohen, H. N. Chapman, J. Miao, and M. Segev, "Phase retrieval with application to optical imaging: a contemporary overview," *IEEE Signal Processing Magazine*, vol. 32, n. 3, pp. 87-109, 2015.

[17] A. F. Morabito, R. Palmeri, V. A. Morabito, A. R. Laganà, and T. Isernia, "Single-surface phaseless characterization of antennas via hierarchically ordered optimizations," *IEEE Transactions on Antennas and Propagation*, vol. 67, n. 1, pp. 461-474, 2018.

[18] T. Isernia, G. Leone, and R. Pierri, "Phase retrieval of radiated fields," *Inverse Problems*, vol. 11, n. 1, p. 183, 1995.

[19] D. L. Misell, "A method for the solution of the phase problem in electron microscopy," *Journal of Physics D: Applied Physics*, vol. 6, n. 1, 1973.

[20] A. R. Laganà, A. F. Morabito, and T. Isernia, "Phase retrieval by constrained power inflation and signum flipping," *Radio Science*, vol. 51, pp. 1855–1863, 2016.

[21] R. Pierri, G. D'Elia, and F. Soldovieri, "A two probes scanning phaseless near-field far-field transformation technique," *IEEE Transactions on Antennas and Propagation*, vol. 47, n. 5, pp. 792–802, 1999.

[22] F. Soldovieri, A. Liseno, G. D'Elia, and R. Pierri, "Global convergence of phase retrieval by quadratic approach," *IEEE Transactions on Antennas and Propagation*, vol. 53, n. 10, pp. 3135-3141, 2005.

[23] T. Isernia, F. Soldovieri, G. Leone, and R. Pierri, "On the local minima in phase reconstruction algorithms," *Radio Science*, vol. 31, n. 6, pp. 1887-1899, 1996.

[24] J. R. Fienup, "Phase retrieval algorithms: A comparison," *Applied Optics*, vol. 21, n. 15, pp. 2758–2769, 1982.

[25] S. Marchesini, "A unified evaluation of iterative projection algorithms for phase retrieval," *Review of scientific instruments*, vol. 78, n. 1, 2007.

[26] D. H. Wolpert, and W. G. Macready, "No free lunch theorems for optimization," *IEEE Transactions on Evolutionary Computation*, vol. 1, n. 1, pp. 67-82, 1997.

[27] B. Fuchs, L. Le Coq, "Excitations retrieval of microwave linear arrays from phaseless far field data", *IEEE Transactions on Antennas and Propagation*, vol. 63, n. 2, pp. 748-752, Feb. 2015.

[28] R. Moretta, R. Pierri, "Performance of Phase Retrieval via Phaselift and quadratic inversion in circular scanning case", *IEEE Transactions on Antennas and Propagation*, vol. 67, n. 12, pp. 7528-7537, Dec 2019.

[29] G. M. Battaglia, R. Palmeri, A. F. Morabito, P. G. Nicolaci, and T. Isernia, "A non-iterative crosswords-inspired approach to the recovery of 2-D discrete signals from phaseless fourier transform data," *IEEE Open Journal of Antennas and Propagation*, vol. 2, pp. 269-280, 2021.

[30] A. F. Morabito, L. Di Donato, and T. Isernia, "Orbital angular momentum antennas: understanding actual possibilities through the aperture antennas theory," *IEEE Antennas and Propagation Magazine*, vol. 60, n. 2, pp. 59-67, 2018.

[31] R. Piessens, "The Hankel transform," in *The Transforms and Applications Handbook*, A. D. Poularikas, Ed. Boca Raton: CRC, 2000.

[32] T. Isernia, O. M. Bucci, and N. Fiorentino, "Shaped beam antenna synthesis problems: feasibility criteria and new strategies," *Journal of Electromagnetic Waves and Applications*, vol. 12, n. 1, pp. 103-138, 1998.

[33] A. F. Morabito, A. Di Carlo, L. Di Donato, T. Isernia, and G. Sorbello, "Extending spectral factorization to array pattern synthesis including sparseness, mutual coupling, and mounting-platform effects," *IEEE Transactions on Antennas and Propagation*, vol. 67, n. 7, pp. 4548-4559, 2019.

[34] G. M. Battaglia, R. Palmeri, A. F. Morabito, and T. Isernia, "A new 'X-words like' approach to two dimensional phase retrieval problems," *15th European Conference on Antennas and Propagation (EuCAP)*, pp. 1-3, 2021.

[35] R. Palmeri, G. M. Battaglia, A. F. Morabito, and T. Isernia, "Phase Retrieval of 2-D Radiated Fields from Phaseless Data: A new Crossword Approach," *2021 Antenna Measurement Techniques Association Symposium (AMTA)*, pp. 1-5, 2021.

[36] M. Bertero, and P. Boccacci, "Singular value decomposition," *Introduction to Inverse Problems in Imaging*, CRC press, pp. 220–246, 1998.

[37] O. M. Bucci, C. Gennarelli, and C. Savarese, "Representation of electromagnetic fields over arbitrary surfaces by a finite and nonredundant number of samples," *IEEE Transaction on Antennas and Propagation*, vol. 46, n. 3, pp. 351-359, 1998.

[38] T. Isernia, G. Leone, R. Pierri, and F. Soldovieri, "Role of support information and zero locations in phase retrieval by a quadratic approach," *Journal of the Optical Society of America A*, vol. 16, n. 7, pp. 1845-1856, 1999.

[39] C. A. Balanis, "Fourier Transforms in Aperture Antenna Theory," *Antenna Theory, Analysis, and Design*, Chapter 12.9, p. 701, 3rd Edition, John Wiley & Sons, Inc., Hoboken, New Jersey, 2005.

[40] S. R. Dooley, A. K. Nandi, "Notes on the interpolation of discrete periodic signals using sinc functions related approaches", *IEEE Transactions on Signal Processing*, vol. 48, n. 4, pp. 1201-1203, 2000.

[41] S. A. Schelkunoff, "A mathematical theory of linear arrays," *The Bell System Technical Journal*, vol. 22, n. 1, pp. 80-107, 1943.

[42] O. M. Bucci, T. Isernia, and A. F. Morabito, "Optimal synthesis of circularly symmetric shaped beams," *IEEE Transactions on Antennas and Propagation*, vol. 62, n. 4, pp. 1954-1964, 2014.

[43] Y. U. Kim, R. S. Elliott, "Shaped pattern synthesis using pure real distributions," *IEEE Transactions on Antennas and Propagation*, vol. 36, n. 11, pp. 1645-1649, Nov 1988.

[44] C. Xiong, G. Xiao, "Excitation retrieval for phased arrays with magnitude-only fields measured at a fixed location," *IEEE Antennas and Wireless Propagation Letters*, vol. 20, n. 2, pp. 264-268, 2021.

[45] R. M. Von Bunau, H. Fukuda, and T. Terasawa, "Phase retrieval from defocused images and its applications in lithography," *Japanese Journal of Applied Physics*, vol. 36, n. 12S, p. 7494, 1997.

[46] A. Grjasnow, A. Wuttig, and R. Riesenberg, "Phase resolving microscopy by multi-plane diffraction detection," *Journal of Microscopy*, vol. 231, n. 1, pp. 115–123, 2008.

[47] O. M. Bucci, G. D'Elia, G. Leone, and R. Pierri, "Far-field pattern determination from the near-field amplitude on two surfaces," *IEEE Transactions on Antennas and Propagation*, vol. 38, n. 11, pp. 1772-1779, 1990.

[48] O. M. Bucci, G. D'Elia, and M. D. Migliore, "An effective near-field far-field transformation technique from truncated and inaccurate amplitude-only data," *IEEE Transactions on Antennas and Propagation*, vol. 47, n. 9, pp. 1377-1385, 1999.

[49] A. Capozzoli, C. Curcio, G. D'Elia, A. Liseno, "Phaseless antenna characterization by effective aperture field and data representations," *IEEE Transactions on Antennas and Propagation*, vol. 57, n. 1, pp. 215-230, 2009.

[50] A. P. Anderson, S. Sali, "New possibilities for phaseless microwave diagnostics - Part I: Error reduction techniques," *IEE Proceedings H - Microwaves, Antennas and Propagation*, vol. 132, n. 5, pp. 291-298, 1985.

[51] R. G. Yaccarino, Y. Rahamat-Samii, "Phaseless bi-polar near field measurements and diagnostics of array antennas," *IEEE Transactions on Antennas and Propagation*, vol. 47, n. 3, pp. 574-583, 1999.

[52] H. B. Curry, "The method of steepest descent for non-linear minimization problems," *Quarterly of Applied Mathematics*, vol. 2, n. 3, pp. 258–261, 1944.

[53] R. Pierri, R. Moretta, "On data increasing in phase retrieval via quadratic inversion: flattening manifold and local minima," *IEEE Transactions on Antennas and Propagation*, vol. 68, n. 12, pp. 8104-8113, 2020.

[54] J. A. López Pérez, P. de Vicente Abad, J. A. Lopez-Fernandez, F. Tercero Martinez, A. Borcia Cancio, B. Galocha Iragüen, "Surface Accuracy Improvement of the Yebes 40 meters radio telescope using microwave holography", *IEEE Transactions on Antennas and Propagation*, vol. 62, n. 5, pp. 2624-2632, 2014.

[55] O. M. Bucci, M. D'Urso, "Power pattern synthesis of given sources exploiting array methods," *Proceedings of the Second European Conference on Antennas and Propagation*, p. 144, Nov 2007.